Available online at www.sciencedirect.com
ScienceDirect
Trans. Nonferrous Met. Soc. China 24(2014) 1779−1784

Transactions of
Nonferrous Metals
Society of China
www.tnmsc.cn

Pyrolysis mechanism of ZrC precursor and fabrication of C/C–ZrC composites by precursor infiltration and pyrolysis

Chun-xuan LIU, Jian-xun CHEN, Zhe-an SU, Xin YANG, Liu-xu CAO, Qing-zhong HUANG

State Key Laboratory of Powder Metallurgy, Central South University, Changsha 410083, China

Received 29 July 2013; accepted 27 February 2014

Abstract: C/C−ZrC composites were prepared by precursor infiltration and pyrolysis using the organic zirconium as precursor. The conversion mechanisms of the precursors such as the thermal behavior, structural evolution, phase composition, microstructure, composition of the precursors and products were analyzed by thermal gravimetric analyzer, Fourier transform infrared spectrometer, X-ray diffraction and scanning electron microscope. The results indicate that the ZrC precursor transforms to inorganic ZrO_2 from room temperature to 1200 °C, then reduces to ZrC at 1600 °C through the carbothermal reduction reaction. The microstructure of the C/C−ZrC composites was also investigated. The composites exhibit an interesting structure, a coating composed of ZrC ceramic covers the exterior of the composite, and the ZrC ceramic is embedded in the pores of the matrix inside the composite.

Key words: ZrC precursor; pyrolysis mechanism; precursor infiltration and pyrolysis; C/C−ZrC composites

---

1 Introduction

Carbon/carbon (C/C) composites have received considerable attentions due to their excellent properties such as high-temperature strength, low coefficient of thermal expansion, high thermal conductivity and outstanding thermal shock resistance [1−3]. However, the rapid oxidation of the composites under high-temperatures has seriously limited their applications [4,5]. Therefore, the improvement of ablation and oxidation resistance of C/C composites has attracted considerable attentions recently.

Silicon carbide can protect carbon/carbon composites from oxidation at relatively lower temperatures. However, silica readily vaporizes when the temperature reaches 1600 °C [6]. Introduction of ultra-high temperature ceramics (UHTCs) into these C/C composites to improve their ablation and erosion resistance is a good method to improve the high-temperature performance [7,8]. Due to its high melting point (3540 °C), good chemical inertness, low evaporation rates, high hardness and good ablation resistance, ZrC is one of the most promising candidates for ultra-high temperature applications to protect C/C composites from ablation and erosion [9,10].

Up to date, various approaches have been developed such as powder doping, chemical vapor infiltration and liquid precursor impregnation, to introduce ZrC into C/C composites, which have been widely studied in previous works. LI et al [11] developed two-dimensional (2D) C/ZrC–SiC composites fabricated by chemical vapor infiltration (CVI) process combined with a modified precursor infiltration and pyrolysis (PIP) method. LI et al [12] reported 2D reinforced C/C−ZrC−SiC composites prepared by isothermal chemical vapor infiltration (ICVI) combined with reactive melt infiltration (RMI) process. LI et al [13] prepared 3D C_f/ZrC−SiC composites through PIP process using a hybrid precursor containing polycarbosilane and organic zirconium polymeric precursor. Various organic zirconium precursors have been used to produce ZrC ceramics. AMOROS et al [14] and YU et al [15] used bis(cyclopentadienyl)-metal dichloride (Cp_2MCl_2) as an alternative source of ZrC to obtain SiC/C/ZrC ceramics. It is revealed that the polymer-to-ceramic conversion was completed at 900 °C obtaining amorphous ZrC ceramic. ZHAO et al [16] used $Zr(OC_4H_9)_4$ and DVB as the zirconia and carbon precursor to produce ZrC containing a small amount of m-ZrO_2.

Foundation item: Project (2011CB605801) supported by the National Basic Research Program of China; Project (CX2012B042) supported by the Graduated Students' Scientific Research Innovation Project in Hunan Province of China

Corresponding author: Qing-zhong HUANG; Tel: +86-731-88836078; E-mail: qzhuang@csu.edu.cn

DOI: 10.1016/S1003-6326(14)63253-2

Although considerable achievements have been acquired in this field, each of these processing methods has disadvantages, such as high cost, difficulty in controlling reaction conditions, and poor performance of the composites. In this work, C/C−ZrC composites with the well-distributed ZrC phase was prepared by PIP using a novel laboratory synthesized organic zirconium precursor. The conversion mechanisms of the precursors such as the thermal behavior, structural evolution, phase composition, microstructure, composition of the precursors and products were investigated.

2 Experimental

2.1 Raw materials and processing

The precursor of organic zirconium (POZ, 29.4% Zr, 51.3% C, 12.6% O, 6.7% H (mass fraction)) was provided by Central South University, China. To investigate the pyrolysis mechanism, POZ was heat treated in a graphite crucible in a high temperature graphite resistance furnace at temperatures ranging from 300 to 2000 °C under vacuum at a rate of 10 °C/min. After pyrolysis, the ceramic was cooled to room temperature in the furnace. The C/C composites were densified to about 1.40 g/cm^3 from carbon fiber performs by CVI with CH_4, H_2 and N_2. The C/C−ZrC composites were fabricated by PIP with the organic zirconium precursor at 1400−1600 °C. The PIP process was repeated for ten times until the density of the C/C−ZrC composites reached about 1.90 g/cm^3.

2.2 Characterization

Thermal analysis of the precursors was investigated with thermal gravimetric analysis (TGA, Netzsch STA 409EP, Netzsch, Germany SDT Q600 V8.0 Build 95) in an argon atmosphere with a heating rate of 10 °C/min from room temperature to 900 °C. Fourier transform infrared spectroscopy (FTIR, Nicolet-6700, Madison, US) analysis was performed on the precursor with KBr plates for liquid samples and KBr discs for solid samples. The phase compositions were characterized using X-ray diffraction (XRD, D/max 2500, Rigaku, Japan) with Cu K_α radiation. Spectra was obtained by scanning from 10° to 85° at 0.02° per step. Scanning electron microscopy (SEM, Nova NanoSEM230, FEI, US) was used to characterize the microstructure of the heat treated samples. An accelerating voltage of 18 kV was used for phase identification to allow for the adequate phase contrast.

3 Results and discussion

3.1 Pyrolysis behavior of precursor

In order to understand the thermal behavior of POZ during the pyrolysis process, TGA was measured and the result is shown in Fig. 1. The TGA curve of the precursor shows two important mass loss steps. The first one is from room temperature to about 200 °C and the second one is at the temperatures between 200 and 380 °C. When the temperature is over 380 °C, the mass appears a steady though slow decrease till 900 °C.

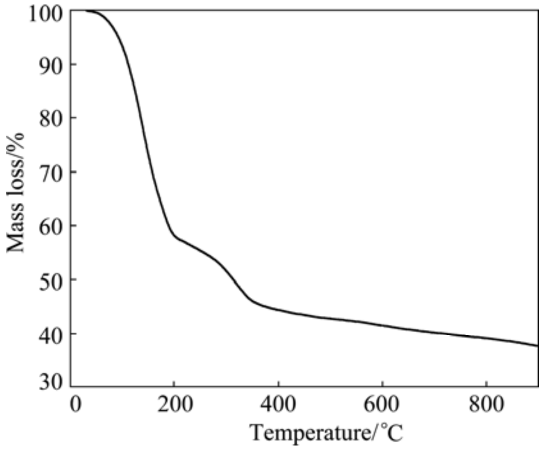

Fig. 1 TGA curves of POZ from room temperature to 900 °C

It is observed that there was about 45% mass loss ratio from room temperature to 200 °C. The other mass loss ratio of 15% at 200−380 °C is due to the completely decomposition of the organic component. At higher temperatures the conversion into the inorganic state goes on and the mass decreases very slowly until the temperature is more than 900 °C. The assumption can be further confirmed by the later results of the structural evolution of POZ. The mass fraction of residual products of POZ reaches about 37.6% at 900 °C.

FTIR spectra of POZ were thus measured from room temperature to 900 °C to study the structural evolution of POZ precursors during the pyrolysis process. Figure 2 shows the FTIR spectra of the POZ sample from room temperature to 900 °C. The peaks at 607 cm^{-1} and 456 cm^{-1} were characteristic of Zr—O and Zr—C bonds, respectively, which exists from room temperature to 900 °C. The absorption peaks at 3062, 2925, 2869, 1453, 1495, 734 and 697 cm^{-1} indicate the existence of benzyl in POZ molecule at room temperature.

After the heat treatment at 300 °C, all the absorption peaks of benzyl are vanished. This phenomenon indicates that most of the organic functional groups of POZ are decomposed at relatively low temperature, which well matches with the TGA results above. When the sample is heated to 900 °C, only the peaks of Zr—O and Zr—C are retained, and other bands such as 3389, 1633 and 1384 cm^{-1} (attributed to —OH) are no longer observed in the FTIR spectrum. It can be tentatively proposed that the conversion of POZ from organic to inorganic is completed below 900 °C. And the

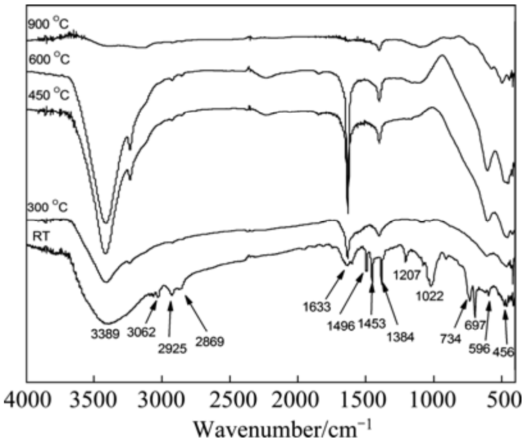

Fig. 2 FTIR spectra of POZ at room temperature and at 300−900 °C

conversion from amorphous to crystalline phase during the heat treatment will be further discussed by XRD analysis.

In order to investigate the crystallization evolution of POZ, XRD patterns of the samples were measured. Figures 3 and 4 show the XRD patterns of the samples obtained by pyrolyzing the precursor of POZ at 300−2000 °C for 60 min, respectively.

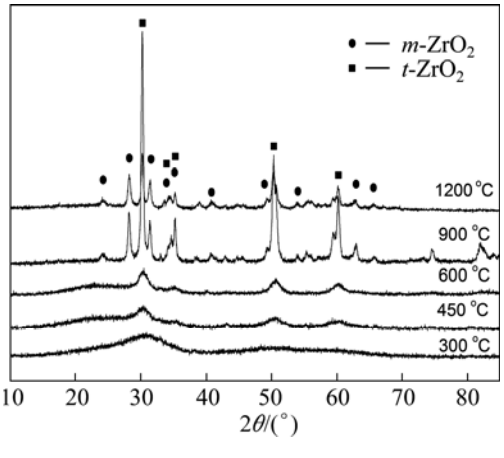

Fig. 3 XRD patterns of POZ after heat treatment at 300−1200 °C

When the precursor is treated at higher temperatures, the phase composition and crystal structure change markedly (Fig. 4). The XRD patterns of this sample show that the ZrC phase is formed at the temperature of 1400 °C. As the heat treatment temperature increases to 1600 °C, ZrC becomes the dominant phase, while the phases of m-ZrO_2 and t-ZrO_2 almost disappear. When the heat treatment temperature increases to 2000 °C, the XRD pattern is basically in agreement with the typical structure ZrC diffraction. There is no characteristic peak related to m-ZrO_2 and t-ZrO_2. And the diffraction peaks are very sharp, indicating the good crystallinity of ZrC.

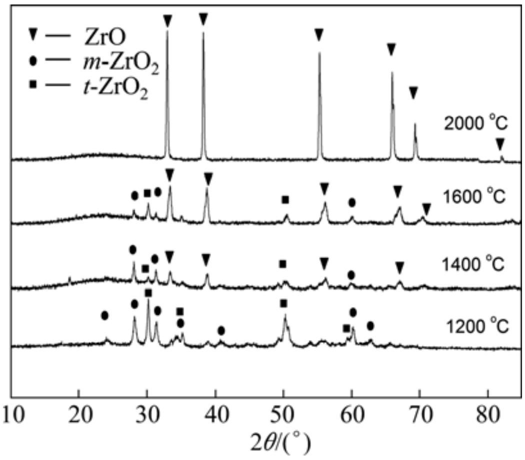

Fig. 4 XRD patterns of POZ after heat treatment at 1200−2000 °C

Microstructures of the ceramics prepared by POZ precursor after heat treatment at 1200−2000 °C are shown in Fig. 5. Figure 5(a) shows that the vast spherical grain of ZrO_2 obviously exists on the surface of the materials. In contrast, when the temperature increases to 1400−2000 °C, the small spherules disappear, and the compactness of the materials is obviously increased. At the same time, the crystallization becomes evident for these products, and the crystallization degree increases with the increasing of temperature. The microstructures of these ZrC ceramics are compact. These observations are consistent with the trends observed in XRD results (Figs. 3 and 4).

It’s assumed that the POZ could be used to produce ZrC ceramics. Combined with the results in this work, the pyrolysis and ceramization process of POZ mainly includes three stages from room temperature to 2000 °C. First, the organic POZ precursor transforms to inorganic ZrO_2 from room temperature to 1200 °C; then ZrO_2 reduces to ZrC from 1200 to 1600 °C through carbothermal reduction reaction; at last, ZrO_2 completely reduces to ZrC, and the ZrC phase basically transforms to crystalline phase from 1600 to 2000 °C. Therefore, the C/C−ZrC composites are prepared by PIP at the reasonable temperature of 1400−1600 °C.

3.2 Microstructure characterization of C/C−ZrC composites

Unlike the C/C−ZrC composites prepared by PIP using other organic zirconium precursors, the C/C−ZrC composites produced in this work show an interesting structure with ZrC coating as the outer layer and the well distributed ZrC as ceramics phase matrix in the C/C composites. The XRD pattern of the C/C−ZrC composites surface is shown in Fig. 6. The strong peaks corresponding to ZrC are detected. It reveals that the surface of the composite is mainly composed of ZrC. No

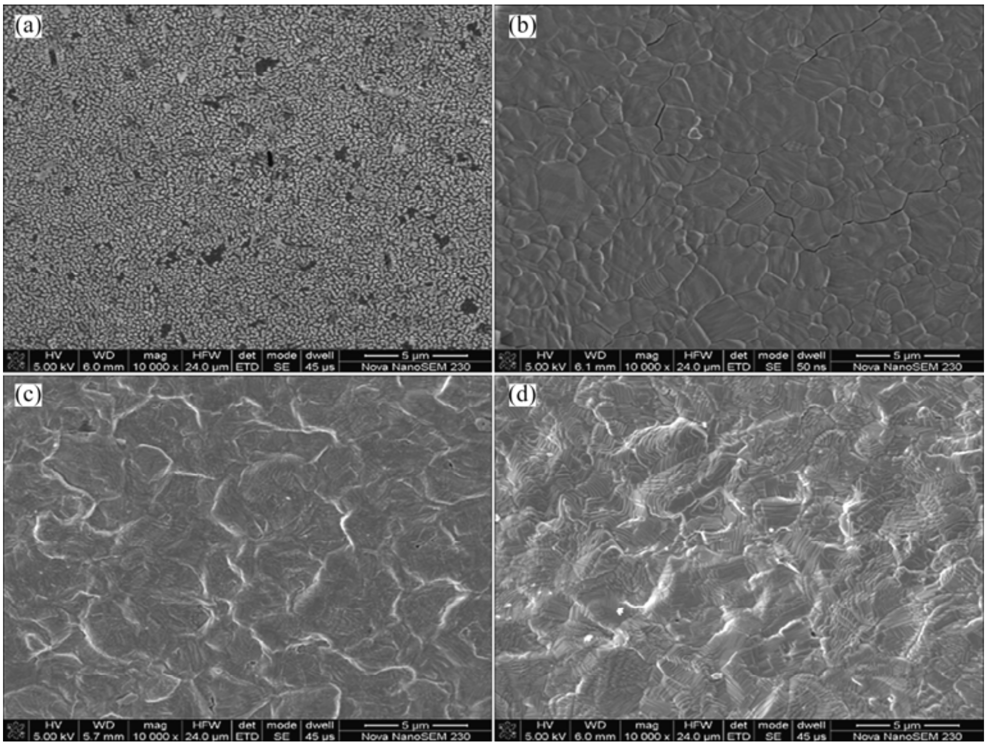

Fig. 5 SEM images of ceramic derived from POZ precursor at different temperatures: (a) 1200 °C; (b) 1400 °C; (c) 1600 °C; (d) 2000 °C

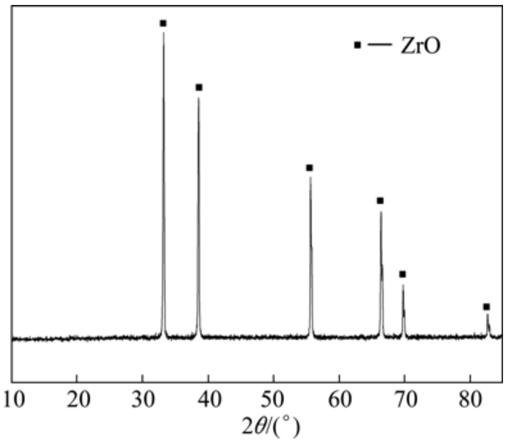

Fig. 6 XRD patterns of surface of composites

detectable C or ZrO_2 peaks are found in the XRD patterns, which may be attributed to the carbothermal reduction reaction of ZrO_2 at about 1600 °C in inert atmosphere to form ZrC ceramics. Meanwhile the existence of pyrolytic carbon in the C/C composites may be beneficial to the carbothermal reduction reaction of ZrO_2.

Figure 7 shows SEM images of the surface of the C/C−ZrC composites. The ceramics grains in different sizes are connected to each other and form a continuous coating on the surface of the composite (Fig. 7(a)). According to the XRD patterns of the composite surface in Fig. 6, the small grains are composed of ZrC. The ZrC

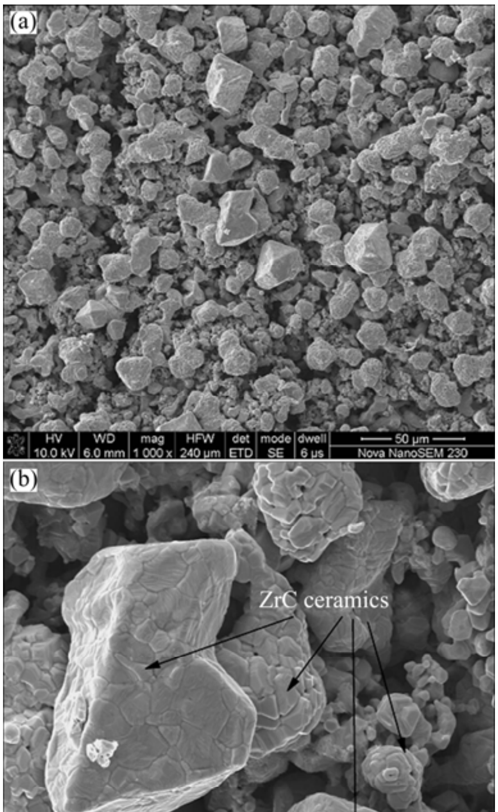

Fig. 7 SEM images of surface morphology of C/C−ZrC composites: (a) Low magnification; (b) High magnification

ceramic coating is very rough, and some holes can be found on the surface. The holes may be produced from the carbothermal reduction reaction consuming some pyrolytic carbon on the surface. To some extent, the ZrC ceramic on the surface of the composites can protect the material from ablation in a high-temperature environment. Figure 7(b) shows the larger magnification of the C/C−ZrC composites. Though the sizes of the ZrC grains are not uniform, the crystallization performance is very excellent.

Figure 8 shows the XRD phase analysis for the cross-section of the composites. Compared with XRD pattern shown in Fig. 6, it can be seen that a new carbon phase is detected in the cross-section of the composites. The peaks of carbon at 26.46° and 44.56° can be indexed as graphitic (002) and (101) planes according to the JCPDS cards No. 41−1487. The phase of ZrC is formed due to the pyrolysis of the organic zirconium precursor and the carbothermal reduction reaction of ZrO_2 with PyC, while the carbon phase is from the carbon fibers or PyC. There is no evidence to suggest that ZrO_2 phase exists in the composites.

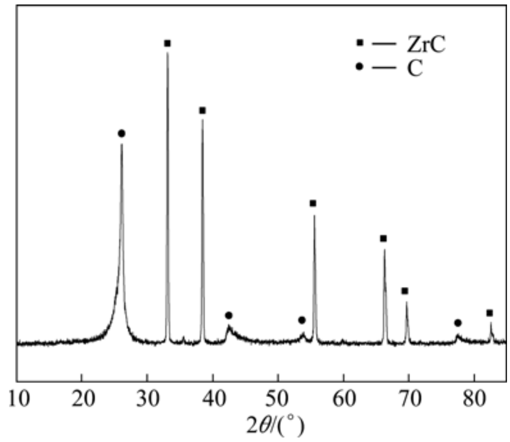

Fig. 8 XRD patterns of cross-section of C/C–ZrC composites

The cross-section microstructure of the C/C−ZrC composites before and after ablation is shown in Fig. 9. As shown in Fig. 9, the ZrC ceramics mainly concentrate in the pores of the composites to fill the holes and grooves, which may provide tunnels for the oxygen diffusion during the ablation process. Therefore, this structure can efficiently protect the composites from ablation. In the PIP process, the organic zirconium precursor infiltrates the apertures of the C/C composite, and then transforms into ZrC ceramics to fill the apertures during the pyrolysis process. Thus, the cross-section of the composite is compact.

According to the SEM and XRD results mentioned above, a possible structure model can be tentatively proposed for the C/C−ZrC composite. A coating composed of ZrC ceramics can be observed on the composite surface, which can protect the composite from ablation during the test. Inside the composite, the ZrC ceramics are embedded in the pores of the matrix. This condition indicates that the small interspaces of the composite are sealed by the ceramics, which can prevent oxygen from ablating the matrix when the out-layer is destroyed in high-temperature environments.

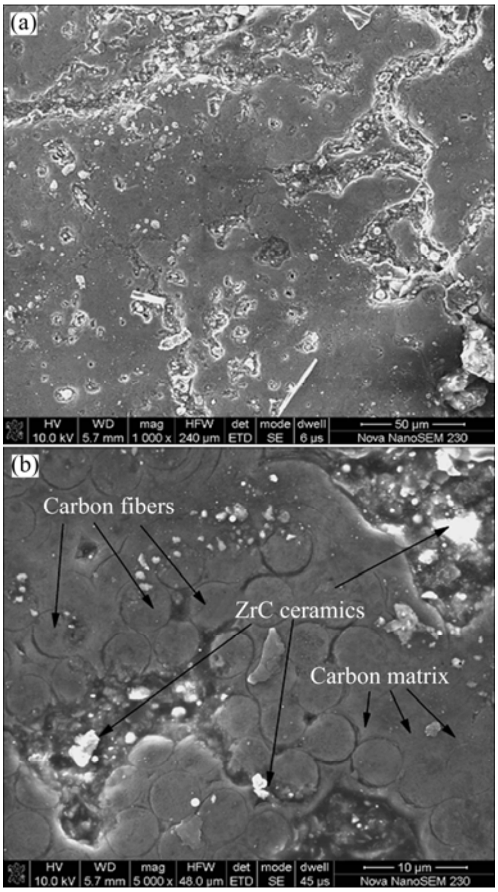

Fig. 9 SEM images of cross-section morphology of C/C−ZrC composites: (a) Low magnification; (b) High magnification

4 Conclusions

1) The transforming mechanism of ZrC from the precursor was investigated by TGA, FTIR, XRD and SEM. The yield of POZ was about 37.6% when the heat-treatment temperature reached 900 °C.

2) The organic POZ precursor transformed to inorganic ZrO_2 from room temperature to 1200 °C, then ZrO_2 reduced to ZrC from 1200 to 1600 °C through carbothermal reduction reaction, at last ZrO_2 completely reduced to ZrC crystalline phase from 1600 to 2000 °C.

3) C/C−ZrC composites were prepared by precursor infiltration and pyrolysis using laboratory synthesized organic zirconium as the precursor. The microstructure of the C/C−ZrC composites indicates that the composites exhibit an interesting structure, wherein a coating composed of ZrC ceramics covers the exterior of the

composite, and the ZrC ceramics are embedded in the pores of the matrix inside the composite.

References

[1] LI J S, LUO R Y. Study of the mechanical properties of carbon nanofiber reinforced carbon/carbon composites [J]. Composites Part A, 2008, 39(11): 1700−1704.

[2] ZHANG M Y, WANG L P, HUANG Q Z, CHAI L Y. Rapid chemical vapor infiltration of C/C composites [J]. Transactions of Nonferrous Metals Society of China, 2009, 19(6): 1436−1439.

[3] ZHANG M Y, SU Z A, LI J L, HUANG Q Z. Bending properties and fracture mechanism of C/C composites with high density preform [J]. Transactions of Nonferrous Metals Society of China, 2011, 21(8): 1795−1800.

[4] JAYASEELAN D D, GUIMARAES S R, BROWN P, LEE W E. Reactive infiltration processing (RIP) of ultra high temperature ceramics (UHTC) into porous C/C composite tubes [J]. Journal of the European Ceramic Society, 2011, 31: 361−368.

[5] SHEEHAN J E. Oxidation protection for carbon fiber composites [J]. Carbon, 1989, 27(5): 709−715.

[6] WANG Z, DONG S M, ZHANG X Y, ZHOU H J, WU D X, ZHOU Q, JIANG D L. Fabrication and properties of C_f/SiC–ZrC composites [J]. Journal of the American Ceramic Society, 2008, 91(10): 3434−3436.

[7] LI Z Q, LI H J, ZHANG S Y, LI K Z. Microstructure and ablation behaviors of integer felt reinforced C/C−SiC−ZrC composites prepared by a two-step method [J]. Ceramics International, 2012, 38(4): 3419−3425.

[8] SHEN X T, LI K Z, LI H J, DU H Y, CAO W F, LAN F T. Microstructure and ablation properties of zirconium carbide doped carbon/carbon composites [J]. Carbon, 2010, 48(2): 344−351.

[9] LIU C, LIU B, SHAO Y L, LI Z Q, TANG C H. Vapor pressure and thermochemical properties of $ZrCl_4$ for ZrC coating of coated fuel particles [J]. Transactions of Nonferrous Metals Society of China, 2008, 18(3): 728−732.

[10] WANG Y J, SONG G M, MENG Q C, ZHOU Y. Strength properties and fracture behavior of ZrC particle-reinforced tungsten composite [J]. Transactions of Nonferrous Metals Society of China, 2001, 11(6): 868−872.

[11] LI H B, ZHANG L T, CHENG L F, WANG Y G. Fabrication of 2D C/ZrC−SiC composite and its structural evolution under high-temperature treatment up to 1800 °C [J]. Ceramics International, 2009, 35: 2831−2836.

[12] LI Z Q, LI H J, ZHANG S Y, WANG J, LI W, SUN F J. Effect of reaction melt infiltration temperature on the ablation properties of 2D C/C−SiC−ZrC composites [J]. Corrosion Science, 2012, 58: 12−19.

[13] LI Q G, DONG S M, WANG Z, HE P, ZHOU H J, YANG J S, WU B, HU J B. Fabrication and properties of 3-D C_f/SiC−ZrC composites, using ZrC precursor and polycarbosilane [J]. Journal of the American Ceramic Society, 2012, 95(4): 1216−1219.

[14] AMOROS P, BELTRAN D, GUILLEM C, LATORRE J. Synthesis and characterization of SiC/MC/C ceramics (M=Ti, Zr, Hf) starting from totally non-oxidic precursors [J]. Journal of Materials Chemistry, 2002, 14: 1585−1590.

[15] YU Z J, YANG L, ZHAN J Y, ZHOU C, MIN H, ZHENG Q, XIA H P. Preparation, cross-linking and ceramization of AHPCS/Cp_2ZrCl_2 hybrid precursors for SiC/ZrC/C composites [J]. Journal of the European Ceramic Society, 2012, 32(6): 1291−1298.

[16] ZHAO D, HU H F, ZHANG C R, ZHANG Y D, WANG J. A simple way to prepare precursors for zirconium carbide [J]. Journal of Materials Science and Technology, 2010, 45: 6401−6405.

碳化锆陶瓷先驱体裂解机理及 PIP 法制备 C/C−ZrC 复合材料

刘春轩，陈建勋，苏哲安，杨 鑫，曹柳絮，黄启忠

中南大学 粉末冶金国家重点实验室，长沙 410083

摘 要：使用有机锆先驱体，通过先驱体高温裂解工艺制备 C/C−ZrC 复合材料。采用热重分析仪、傅里叶转换红外光谱、X 射线衍射、扫描电子显微镜等手段研究该有机锆先驱体高温裂解过程中的热失重行为、官能团的转变情况、物相转化过程及显微组织。结果表明：有机锆先驱体从室温加热至 1200 °C 时，首先生成无机态的二氧化锆，当裂解温度升高至 1600 °C 时，二氧化锆通过碳热还原反应生成碳化锆陶瓷。对 C/C−ZrC 复合材料的显微组织观察表明，所制备的复合材料具有较好的结构特征：该复合材料的外表面形成一层碳化锆陶瓷层，复合材料内部的大部分孔隙由碳化锆陶瓷基填充。

关键词：ZrC 先驱体；裂解机理；先驱体浸渍−裂解法；C/C−ZrC 复合材料

(Edited by Chao WANG)